



Technical note

Mitochondrial isolation, cryopreservation and preliminary biochemical characterisation from placental cytotrophoblast and syncytiotrophoblast



Joshua J. Fisher, Daniel R. McKeating, Evan N. Pennell, James S. Cuffe, Olivia J. Holland, Anthony V. Perkins*

School of Medical Science, Griffith University, Gold Coast Campus, Southport, 9726, Queensland, Australia

ARTICLE INFO

Keywords:

Syncytiotrophoblast
Mitochondrial isolation
Bioenergetics
Cryopreservation

1. Introduction

The placenta consists of multiple cell layers, including the underlying cytotrophoblast layer and a multi-nucleated, terminally differentiated syncytiotrophoblast. These two cell types possess mitochondria with unique properties; differing in size, morphology, energy production and steroidogenic capacity [1–3]. Mitochondria are vital to virtually every aspect of cellular function from supplying energy in the form of ATP, processing metabolic intermediates, modulating Ca^{2+} signalling, controlling ROS production and playing a critical anabolic role. Many studies have shown that mitochondrial dysfunction contributes to placental pathology underpinning gestational disorders [4,5]. However, due to the complex cell structure of the placenta and the very different biology of cytotrophoblast and syncytiotrophoblast, mitochondrial populations from both are often studied together so subtle variations are missed. One of the key challenges to date has been the development of methodologies for isolation of functional mitochondria that allow key parameters to be assessed in an efficient and reproducible way [3]. Therefore, the aim of this study was to develop methodologies for the isolation, cryopreservation and biochemical analysis of mitochondria from both cytotrophoblast and the syncytiotrophoblast.

2. Methods

2.1. Placental collection and mitochondrial isolation

Ethical approval was granted by both Queensland Health and

Griffith University. Placentae were from healthy term pregnancies, post vaginal birth, and villous tissue was collected as previously described [6]. Isolation of mitochondrial subpopulations was achieved by differential centrifugation adapted from Martinez et al. [3]. Samples were homogenised in a glass dounce homogenizer with 1 mL of chilled isolation media (250 mM sucrose, 0.5 mM Na_2EDTA , 10 mM Tris, pH 7.4). Homogenates were centrifuged at 1,500 g for 10 min at 4 °C and the supernatant collected and centrifuged at 4,000 g for 15 min at 4 °C to produce a pellet of enriched mitochondria (Fraction 1 or Cyto-Mito). The supernatant was collected and centrifuged at 12,000 g for 15 min at 4 °C to produce a second pellet of enriched mitochondria (Fraction 2 or Syncytio-Mito). As the isolation media is designed to allow for cryopreservation of extracted samples, both fractions were analysed fresh or snap frozen and stored at –80 °C. Cryopreserved isolates were revived by warming to 37 °C for 5 min, prior to assessment of mitochondrial respiration. For measurement of mitochondrial membrane potential and ATP production, isolates were revived from storage at –80 °C up to five months later.

2.2. Transmission electron microscopy

Placental tissues were pre-fixed in 3% glutaraldehyde and post-fixed in 1% osmium tetroxide, dehydrated in ethanol, embedded in Epon resin using the Pelco Biowave fixation system and polymerised overnight at 60 °C. Tissue blocks were sectioned (80 nm) using a Leica Ultracut UC6 ultramicrotome and imaged utilising a Joel JSM1011 transmission electron microscope with an Olympus Morada digital camera. Isolated mitochondrial fractions were fixed in 3%

* Corresponding author. School of Medical Science, Griffith University, Gold Coast Campus, Parklands Drive, Southport, QLD, 9726, Australia.
E-mail address: a.perkins@griffith.edu.au (A. Perkins).

glutaraldehyde in mitochondrial isolation buffer, centrifuged to create a cell pellet that was processed and imaged as described for placental tissue. The number of mitochondria were counted, and mitochondrial length measured, and mitochondria classified as large ($\geq 0.2\mu\text{m}$) or small ($\leq 0.1\mu\text{m}$). Ratio of large to small was used to assess % purity.

2.3. Real time respirometry and ATP measurements

Mitochondrial respiration was measured at 37 °C via Oxygraph-2k (OROBROS, Innsbruck, Austria) using the Substrate-Uncoupler-Inhibitor-Titration (SUIT) protocol. Mitochondrial fractions were added in MiRO5 respiration media (0.5 mM EGTA, 3 mM $\text{MgCl}_2 \cdot 6\text{H}_2\text{O}$, 60 mM K-lactobionate, 20 mM taurine, 10 mM KH_2PO_4 , 20 mM HEPES, 110 mM sucrose, 1 g/L fatty acid free BSA, pH 7.1) for baseline calibration (5mins) prior to the sequential addition of Glutamate (10 mM), Malate (2 mM), Pyruvate (5 mM), ADP (1–5 mM) followed by the addition of cytochrome C and Succinate (10 mM) to activate Complex I + II linked respiration and assess mitochondrial membrane integrity, Carbonyl cyanide m-chlorophenyl hydrazone (CCCP; 1 mM) to measure Maximum respiratory capacity. Complex I and III inhibition with Rotenone (1 μM) and Antimycin A (5 mM) respectively, provided measurement of non-mitochondrial respiration. Non-mitochondrial respiration was subtracted from all obtained values to normalise for solely mitochondrial respiration. Respiratory rates were recorded via OROBOROS DataLab 7.0 software and units of respiration are expressed as $\text{pmol O}_2/\text{sec}$ per mg protein. The level of ATP was quantified, after removal of contaminating proteins, utilising an ATP Assay Kit (Abcam, Australia) following the manufacturer's instructions. ATP content was expressed as $\mu\text{mole}/\text{mg}$ of mitochondrial extract.

2.4. Flow cytometry measurement of membrane potential

Following revival mitochondrial isolates were incubated 100 nM MitoSPY Green (Biolegend, United States) and 50 nM TMRE (tetramethylrhodamine, ethyl ester) for 25 min at 37 °C before centrifugation at appropriate speed and resuspension in PBS. Median fluorescence intensity was measured on a BD SORP LSR II Fortessa flow cytometer (BD Biosciences, United States) with identification a minimum of 50,000 fluorescent positive events. Fluorescence Minus One was utilised to establish appropriate gating controls and the intrinsic autofluorescence of unlabelled mitochondria was taken into account [7]. Data was analysed with FlowJo V10 software (FlowJo LLC).

2.5. Statistical analysis

Data is presented as mean \pm SD, with the exception Median Fluorescent Intensity (MFI) for flow cytometry. Analyses were performed using GraphPad PRISM 7.02 (GraphPad, USA), with Student T tests and two-way ANOVA used to determine significance.

3. Results and discussion

As shown in Fig. 1A, mitochondria from cytotrophoblast cells were generally round or ovoid, larger (0.2 μm up to 0.8 μm) with clearly defined cristae (Fig. 1B). Syncytiotrophoblast mitochondria were smaller (0.1 μm or less) with less cristae evident (Fig. 1C). Isolation by differential centrifugation yielded mitochondrial subpopulations of high purity (85–95%), which maintained morphology similar to mitochondria in situ, with no apparent damage induced by centrifugation.

Mitochondrial respiratory capacity was evaluated immediately after isolation and after cryopreservation. Leak state respiration (Fig. 2A) was significantly greater in Cyto-Mito ($p = 0.0028$) than Syncytiotrophoblast. Although it appears that isolated mitochondria from both cell lineages have low leak state respiration, it subsequently increased significantly with addition of substrates (17.5 fold for Cyto-Mito and 20 fold for Syncytiotrophoblast). Complex I + II linked respiration (CI + II;

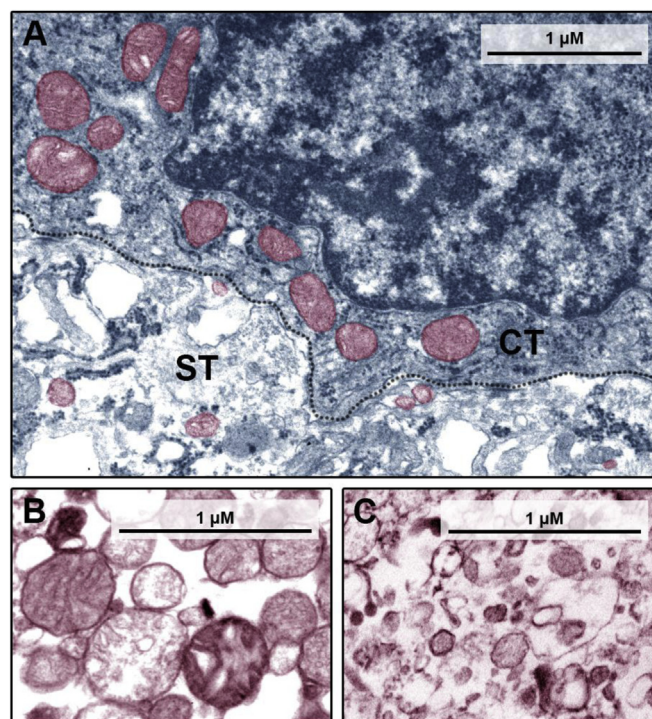


Fig. 1. Placental mitochondria in cytotrophoblasts (CT) and the syncytiotrophoblast (ST). Representative transmission electron microscope images of (A) intact villous placental tissue and isolated mitochondria in Fraction 1 (B) and Fraction 2 (C). Mitochondria were false coloured and a dotted line added to visually separate the cell lineages to aid in identification.

Fig. 2B), and maximum respiratory capacity (Fig. 2C) were significantly higher in Cyto-mito when compared to Syncytiotrophoblast (CI + II: fold change = 2.50, $p = 0.0002$; Max Res Cap. fold change = 2.36, $p = 0.002$). The changes in isolated mitochondria observed in this study supports the existing literature from isolated trophoblast cells, which concluded that cytotrophoblast have a higher respiration rate than syncytiotrophoblast [8]. Further, it has been long established that changes in the cristae structure affect bioenergetics [9], and this may explain the lower bioenergetic capacity of Syncytiotrophoblast. Furthermore, alterations in respirasome complexes and ATP synthase have been associated with altered mitochondrial ultrastructure in the placenta [2]. This study also found that mitochondrial membrane potential was significantly lower in Syncytiotrophoblast ($p = 0.02$) compared to Cyto-Mito and this was reinforced by a significant drop in ATP production ($p = 0.0016$).

Leak state respiration (without the addition of ADP) was similarly maintained and not significantly affected by the cryopreservation. Respiration and maximum respiratory capacity were not significantly different between cryopreserved mitochondrial fractions and fresh isolates, with recovery of respiratory rates between 83 and 93% of freshly isolated mitochondria. As was the case for fresh isolates, CI + II respiration and maximum respiratory capacity were lower in Syncytiotrophoblast compared to Cyto-Mito (Fig. 2B; CI + II: fold change 2.36, $p = 0.0011$; Fig. 2C; Max Res Cap. fold change 2.14, $p = 0.0009$). Evaluation of the outer mitochondrial membrane via exogenous cytochrome c (Figure D) showed an increase in respiration of only 2% in the cryopreservation isolates compared to fresh isolates, while maintaining the ability to determine significance between Cyto-Mito and Syncytiotrophoblast ($p = 0.0023$ fresh and $p = 0.0025$ frozen). These findings suggest that cryopreservation did not have any significant effect on mitochondrial outer membrane integrity. This result is important as when considered in conjunction with membrane potential and ATP production (Fig. 2, E, F) it confirms that the inner mitochondrial membrane was

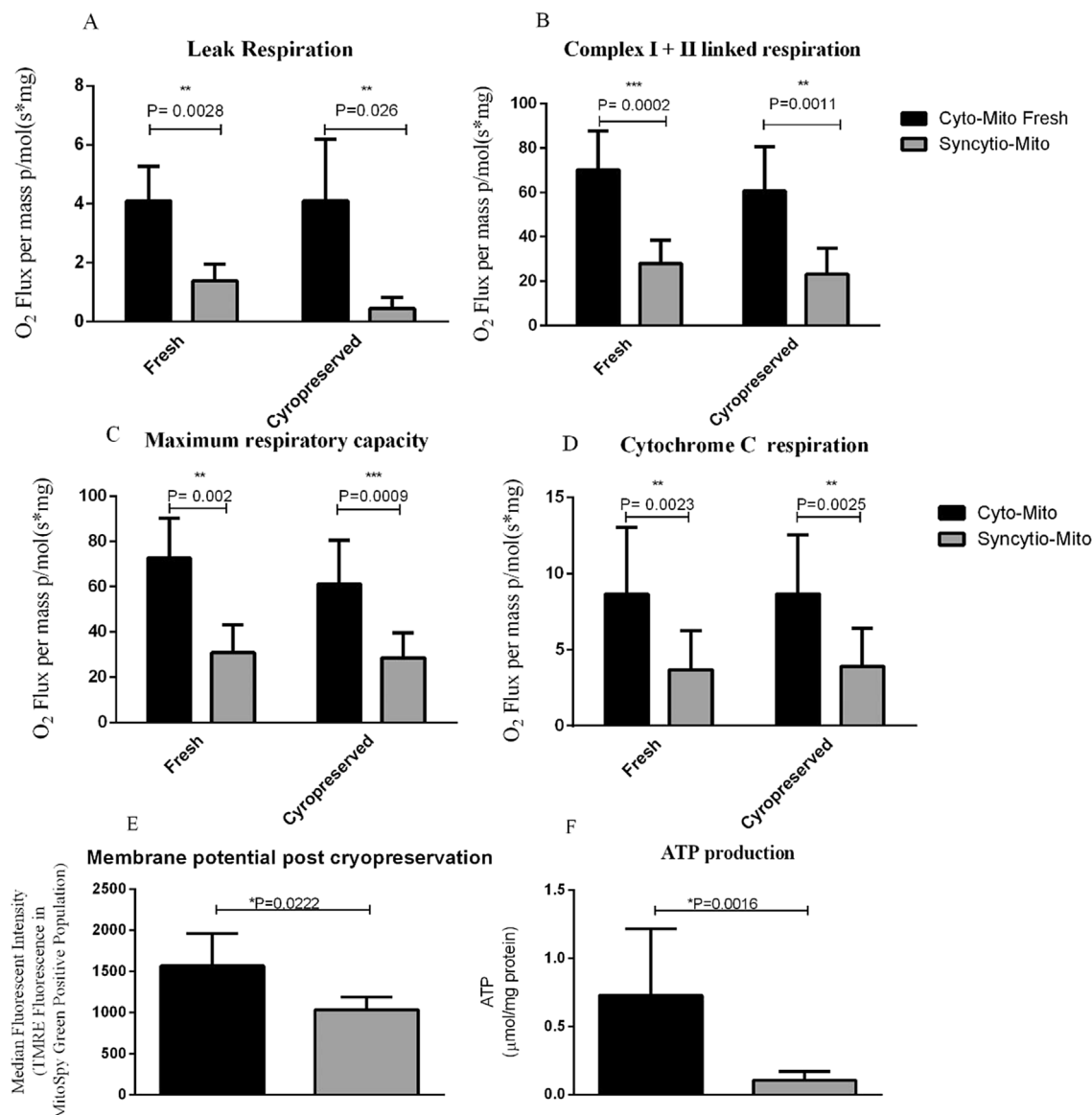


Fig. 2. Mitochondrial respiration, membrane potential and ATP production in fresh and cryopreserved mitochondria from cytotrophoblast (Cyto-Mito (Black bars)) and syncytiotrophoblast mitochondria (Syncytio-Mito (Grey bars)). A) Leak Respiration (n = 7). B) Complex I + II linked respiration (n = 7). C) Maximum respiratory capacity (n = 7). D) Cytochrome C dependent respiration (n = 7). E) Mitochondrial membrane potential post cryopreservation (n = 5). F) ATP production post cryopreservation (n = 9). All data is presented as mean \pm SD with exception of E which is presented as median \pm SD, and n is the number of individual placentae studied.

protected and functioning. The constituents of the isolation buffer aids in the functional recovery post cryopreservation through the use of sucrose, which preserves physiological osmolarity and prevents the loss of matrix ions, protecting the mitochondria from swelling and lysis [10,11].

When comparing our results to that of other human mitochondrial experiments, the placenta has a lower capacity for oxidative phosphorylation than skeletal muscle and cardiac tissue but may be equivalent to that of the liver [12–14]. These comparisons highlight the need to assess mitochondrial subpopulations when examining bioenergetics as respiration rates can change between tissue or even mitochondrial sub populations with a single tissue such as placenta. This research demonstrates the ability to cryopreserve isolated mitochondria at -80°C , without changes in key functional parameters. This will facilitate the study of placental mitochondria from normal and abnormal pregnancies.

Acknowledgements

The Authors would like to acknowledge the facilities and technical assistance of Microscopy Australia, Centre for Microscopy and Microanalysis, University of Queensland.

References

- [1] O. Holland, M. Dekker Nitert, L.A. Gallo, M. Vejzovic, J.J. Fisher, A.V. Perkins, Review: placental mitochondrial function and structure in gestational disorders, *Placenta* 54 (2017) 2–9.
- [2] D. De los Ríos Castillo, M. Zarco-Zavala, S. Olvera-Sanchez, J.P. Pardo, O. Juarez, F. Martinez, G. Mendoza-Hernandez, J.J. García-Trejo, O. Flores-Herrera, Atypical cristae morphology of human syncytiotrophoblast mitochondria: role for complex V, *J. Biol. Chem.* 286 (27) (2011) 23911–23919.
- [3] F. Martinez, M. Kiriakidou, J.F. Strauss 3rd, Structural and functional changes in mitochondria associated with trophoblast differentiation: methods to isolate enriched preparations of syncytiotrophoblast mitochondria, *Endocrinology* 138 (5) (1997) 2172–2183.
- [4] E. Teran, I. Hernández, L. Tana, S. Teran, C. Galaviz-Hernandez, M. Sosa-Macias,

- G. Molina, A. Calle, Mitochondria and coenzyme Q10 in the pathogenesis of pre-eclampsia, *Front. Physiol.* 9 (2018) 1561–1561.
- [5] C. Mandò, G.M. Anelli, C. Novielli, P. Panina-Bordignon, M. Massari, M.I. Mazzocco, I. Cetin, Impact of obesity and hyperglycemia on placental mitochondria, *Oxidative Med. Cell. Longevity* 2018 (2018) 2378189–2378189.
- [6] G.J. Burton, N.J. Sebire, L. Myatt, D. Tannetta, Y.L. Wang, Y. Sadovsky, A.C. Staff, C.W. Redman, Optimising sample collection for placental research, *Placenta* 35 (1) (2014) 9–22.
- [7] S. Dingley, K.A. Chapman, M.J. Falk, Fluorescence-activated cell sorting analysis of mitochondrial content, membrane potential, and matrix oxidant burden in human lymphoblastoid cell lines, *Methods Mol. Biol.* 837 (2012) 231–239.
- [8] K.S. Kolahi, A.M. Valent, K.L. Thornburg, Cytotrophoblast, not syncytiotrophoblast, dominates glycolysis and oxidative phosphorylation in human term placenta, *Sci. Rep.* 7 (2017) 42941.
- [9] C.R. Hackenbrock, Ultrastructural bases for metabolically linked mechanical activity in mitochondria. I. Reversible ultrastructural changes with change in metabolic steady state in isolated liver mitochondria, *J. Cell Biol.* 30 (2) (1966) 269–297.
- [10] J. Nedergaard, B. Cannon, [1] Overview—Preparation and Properties of Mitochondria from Different Sources, *Methods in Enzymology*, Academic Press, 1979, pp. 3–28.
- [11] J.M. Skehel, Preparation of Extracts from Animal Tissues, *Protein Purification Protocols*, Springer, 2004, pp. 15–20.
- [12] E. Gnaiger, Capacity of oxidative phosphorylation in human skeletal muscle: new perspectives of mitochondrial physiology, *Int. J. Biochem. Cell Biol.* 41 (10) (2009) 1837–1845.
- [13] H. Lemieux, S. Semsroth, H. Antretter, D. Höfer, E. Gnaiger, Mitochondrial respiratory control and early defects of oxidative phosphorylation in the failing human heart, *Int. J. Biochem. Cell Biol.* 43 (12) (2011) 1729–1738.
- [14] C. Koliaki, J. Szendroedi, K. Kaul, T. Jelenik, P. Nowotny, F. Jankowiak, C. Herder, M. Carstensen, M. Krausch, W.T. Knoefel, M. Schlensak, M. Roden, Adaptation of hepatic mitochondrial function in humans with non-alcoholic fatty liver is lost in steatohepatitis, *Cell Metabol.* 21 (5) (2015) 739–746.